International Journal of Thermophysics, Vol. 28, No. 1, February 2007 (© 2007)
DOI: 10.1007/s10765-007-0146-6

Deformation due to Mechanical and Thermal Sources in a Thermoelastic Body with Voids under Axi-symmetric Distributions

Rajneesh Kumar[1,2] and Leena Rani[2,3]

Received: April 4, 2005

The Laplace and Hankel transforms have been employed to find the general solution of a homogeneous, isotropic, thermoelastic half-space with voids for a plane axi-symmetric problem. The application of a thermoelastic half-space with voids subjected to a normal force and a thermal source acting at the origin has been considered to show the utility of the solution obtained. To obtain the solution in a physical form, a numerical inversion technique has been applied. The results in the form of displacements, stresses, temperature distribution, and change in volume fraction field are computed numerically and illustrated graphically for a magnesium crystal-like material to depict the effects of voids in the theory of coupled thermoelasticity (CT) and uncoupled thermoelasticity (UCT) for an insulated boundary and a temperature gradient boundary.

KEY WORDS: axi-symmetric problem; Laplace and Hankel transforms; mechanical and thermal sources; thermoelastic; voids.

1. INTRODUCTION

The theory of linear elastic materials with voids is one of the most important generalizations of the classical theory of elasticity. This theory has practical utility for investigating various types of geological and biological materials for which elastic theory is inadequate. This theory is concerned

[1] Mathematics Department, Kurukshetra University, Kurukshetra 136119, Haryana, India.
[2] To whom correspondence should be addressed. E-mail: rajneesh_kuk@rediffmail.com, leena_kkr@rediffmail.com
[3] M. M. Engineering College, Mullana (Ambala) 133203, Haryana, India.

with elastic materials consisting of a distribution of small pores (voids), in which the void volume is included among the kinematic variables and in the limiting case of the volume tending to zero, the theory reduces to the classical theory of elasticity.

A nonlinear theory of elastic materials with voids was developed by Nunziato and Cowin [1]. Later, Cowin and Nunziato [2] developed a theory of linear elastic materials with voids for the mathematical study of the mechanical behavior of porous solids. They considered several applications of the linear theory by investigating the response of the materials to homogeneous deformations, pure bending of beams, and small amplitudes of acoustic waves. Puri and Cowin [3] studied the behavior of plane waves in linear elastic materials with voids. The domain of influence theorem in the linear theory of elastic materials with voids was discussed by Dhaliwal and Wang [4]. Scarpetta [5] studied well-posedness theorems for linear elastic materials with voids. Birsan [6] established the existence and uniqueness of weak solution in the linear theory of elastic shells with voids. Ciarletta et al. [7] studied the stress analysis for cracks in elastic materials with voids.

Rusu [8] studied the existence and uniqueness in thermoelastic materials with voids. Saccomandi [9] presented some remarks about the thermoelastic theory of materials with voids. Ciarletta and Scalia [10] discussed the nonlinear theory of non-simple thermoelastic materials with voids. Ciarletta and Scarpetta [11] discussed some results on thermoelasticity for dielectric materials with voids. Dhaliwal and Wang [12] developed a heat-flux dependent theory of thermoelasticity with voids. Marin [13,14] studied the uniqueness and domain of influence results in thermoelastic bodies with voids. Marin [15] presented the contributions on uniqueness in thermoelastodynamics on bodies with voids. Marin and Salca [16] obtained the relation of the Knopoff-de Hoop type in thermoelasticity of dipolar bodies with voids. Chirita and Scalia [17] studied the spatial and temporal behavior in the linear thermoelasticity of materials with voids. Pompei and Scalia [18] studied the asymptotic spatial behavior in the linear thermoelasticity of materials with voids. Scalia et al. [19] discussed the behavior of steady time harmonic oscillations in thermoelastic materials with voids.

The thermoelastic response of a cylinder in the generalized dynamical theory of thermoelasticity has been studied by Wadhawan [20]. Ghosen and Sabbaghia [21] studied the quasi-static coupled problems of thermoelasticity for cylindrical regions. Chattopadhyay et al. [22] discussed the coupled thermoelastic problem for an infinite aelotropic medium having a cylindrical hole. The thermoelastic transient response of an infinitely long annular cylinder was discussed by Yang et al. [23]. Noda [24] discussed the transient thermoelastic contact problem in a cylinder with a

position-dependent heat transfer coefficient. Kurashige [25] obtained the thermal stresses in a fluid-saturated poroelastic hollow cylinder. Chandrasekharaiah and Keshavan [26] investigated the axi-symmetric thermoelastic interactions in an unbounded body with a cylindrical cavity. Ezzat [27] discussed the fundamental solutions in thermoelasticity with two relaxation times for cylinder regions. Khomasuridze and Khomasuridze [28] studied two-dimensional problems of thermoelasticity in cylindrical and rectangular co-ordinates. Yevtushenko and Kulchysky-Zhyhailo [29] obtained an axi-symmetric steady-state contact problem for thermosensible heated bodies. Mukhopadhyay and Mukherjee [30] investigated the thermoelastic interactions in a transversely isotropic cylinder subjected to a ramp-type increase in the boundary temperature and load. Rahman [31] obtained the axi-symmetric contact problem of thermoelasticity in the presence of an internal heat source. Yanyutin and Yanchevsky [32] studied the identification of an impulsive load acting on an axi-symmetrical hemispherical shell. Sherief et al. [33] discussed generalized thermoelastic problems for an infinitely long hollow cylinder for short times. Baksi et al. [34] explained the eigenvalue approach to study the effect of rotation and relaxation time in two-dimensional problems of generalized thermoelasticity. Kumar and Rani [35] discussed the deformation due to mechanical and thermal sources in a generalized thermoelastic half-space with voids.

In this article, we consider the two-dimensional axi-symmetric problem to determine the components of displacement, stress, temperature distribution, and change in volume fraction field in a homogeneous, isotropic, thermoelastic half-space with voids due to a normal force and thermal source.

2. BASIC EQUATIONS

Following Nowacki [36] and Cowin and Nunziato [2], the field equations and constitutive relations in a thermoelastic solid with voids without body forces, heat sources, and an extrinsic equilibrated body force can be written as

$$\mu\nabla^2\mathbf{u} + (\lambda+\mu)\,\nabla(\nabla\cdot u) + b\nabla\phi - \beta\nabla T = \rho\ddot{\mathbf{u}}, \tag{1}$$

$$\alpha\nabla^2\phi - b(\nabla\cdot u) - \xi_1\phi - \omega_0\dot{\phi} + mT = \rho\chi\ddot{\phi}, \tag{2}$$

$$K\nabla^2 T - \beta T_0(\nabla\cdot\dot{\mathbf{u}}) - mT_0\dot{\phi} = \rho c_e\dot{T}, \tag{3}$$

and

$$t_{ij} = \lambda u_{G,G}\delta_{ij} + \mu(u_{i,j} + u_{j,i}) + (b\phi - \beta T)\ \delta_{ij}, \quad (i, j = x, y, z). \tag{4}$$

where λ and μ are Lame's constants; α, b, ξ_1, ω_0, m, and χ are material constants due to the presence of voids; T is the temperature change; $\beta = (3\lambda + 2\mu)\,\alpha_t$; α_t is the linear thermal expansion; $\mathbf{u}$ is the displacement vector; t_{ij} is the stress tensor, ρ and c_e are the density and specific heat at constant strain, respectively; K is the thermal conductivity, ϕ is the change in volume fraction field, δ_{ij} is the Kronecker delta, T_0 is the uniform temperature; a superposed dot represents differentiation with respect to time variable t; and ∇ and ∇^2 are the gradient and Laplacian operators, respectively.

3. FORMULATION OF THE PROBLEM

We consider a homogeneous, isotropic, thermally conducting elastic half-space with voids in the undeformed state at uniform temperature T_o. The cylindrical polar co-ordinate system (r,θ,z) having an origin on the plane surface $z = 0$ with the z-axis pointing vertically into the medium is introduced. As the problem considered is plane axi-symmetric, i.e., the field component u_θ is zero and u_r, u_z, and T are independent of θ. A normal force or thermal source is assumed to be acting at the origin of the cylindrical polar co-ordinates.

Since the problem considered is plane axi-symmetric, we assume

$$\mathbf{u} = (u, 0, w, t) \tag{5}$$

in Eqs. (1)–(4) where u and w are the radial and vertical components of $\mathbf{u}$.

The initial conditions and regularity are given by

$$\begin{aligned} u(r, z, 0) &= 0 = \dot{u}(r, z, 0), \\ w(r, z, 0) &= 0 = \dot{w}(r, z, 0), \\ \phi(r, z, 0) &= 0 = \dot{\phi}(r, z, 0), \end{aligned}$$

$$T(r, z, 0) = 0 = \dot{T}(r, z, 0) \quad \text{for } z \geq 0,\ 0 \leq r < \infty, \text{ and} \tag{6}$$

$$u(r, z, t) = w(r, z, t) = \phi(r, z, t) = T(r, z, t) = 0 \quad \text{for } t > 0 \text{ when } z \to \infty. \tag{7}$$

We consider mechanical and thermal boundary conditions as

$$\begin{aligned} (1) \quad t_{zz}(r, z, t) &= -P(r, t), t_{zr}(r, z, t) = 0, \\ \frac{\partial \phi}{\partial z} &= 0, \frac{\partial T}{\partial z} + hT = 0 \quad \text{at } z = 0, \end{aligned} \tag{8}$$

where h is the heat transfer coefficient.

$$\begin{aligned}(2)\quad & t_{zz}=0, \quad t_{zr}=0, \quad \tfrac{\partial\phi}{\partial z}=0 \quad \text{at } z=0\\ & \tfrac{\partial T}{\partial z}(r,z,t) = P(r,t) \quad \text{at } z=0, \text{ for the temperature gradient boundary, or}\\ & T(r,z,t)=P(r,t) \quad \text{at } z=0, \text{ for the temperature input boundary.}\end{aligned} \tag{9}$$

4. SOLUTION OF THE PROBLEM

To transform Eqs. (1)–(4) to dimensionless form, we define the following variables:

$$\begin{aligned}& r'=\frac{\omega_1^*}{c_1}r, \quad z'=\frac{\omega_1^*}{c_1}z, \quad t'=\omega_1^* t, \quad u'=\frac{\omega_1^*}{c_1}u, \quad w'=\frac{\omega_1^*}{c_1}w, \quad T'=\frac{T}{T_0},\\ & \phi'=\frac{\omega_1^{*2}\chi}{c_1^2}\phi, \quad \in_1=\frac{\beta c_1^2}{K\omega_1^*}, \quad a'=\frac{\omega_1^*}{c_1}a,\end{aligned} \tag{10}$$

$$t'_{zz}=\frac{t_{zz}}{\beta T_0}, \quad t'_{zr}=\frac{t_{zr}}{\beta T_0}, \quad h'=\frac{hc_1}{\omega_1^*}, \tag{11}$$

where

$$c_1=\left(\frac{\lambda+2\mu}{\rho}\right)^{\frac{1}{2}} \text{ and } \omega_1^*=\frac{\rho c_e c_1^2}{K}.$$

The displacement components can be written as

$$u=\frac{\partial\psi_1}{\partial r}+\frac{\partial^2\psi_2}{\partial r\partial z}, \quad w=\frac{\partial\psi_1}{\partial z}-\left(\nabla^2-\frac{\partial^2}{\partial z^2}\right)\psi_2, \tag{12}$$

where $\psi_1(r,z,t)$and $\psi_2(r,z,t)$ are scalar potential functions.

Applying the Laplace and Hankel transforms,

$$\begin{aligned}& \hat{f}\,(r,z,p)=\int_0^\infty f\,(r,z,t)\,\mathrm{e}^{-pt}\,\mathrm{d}t \text{ and}\\ & \tilde{f}\,(\xi,z,p)=\int_0^\infty \hat{f}\,(r,z,p)\,r J_n(r\xi)\,\mathrm{d}r\end{aligned} \tag{13}$$

on Eqs. (1)–(3); after using Eqs. (10) and (12) (suppressing the primes for convenience)

and eliminating $\tilde{\psi}_1, \tilde{\phi}, \tilde{T}$, and $\tilde{\psi}_2$ from the resulting expressions, we obtain

$$\left(\frac{\mathrm{d}^6}{\mathrm{d}z^6}+Q\frac{\mathrm{d}^4}{\mathrm{d}z^4}+N\frac{\mathrm{d}^2}{\mathrm{d}z^2}+I\right)\left(\tilde{\psi}_1,\tilde{\phi},\tilde{T}\right)=0, \tag{14}$$

and

$$\left(\frac{\mathrm{d}^2}{\mathrm{d}z^2} - \lambda_4^2\right)\tilde{\psi}_2 = 0, \tag{15}$$

where Q, N, I are given in Appendix A.

The roots of Eqs. (14) and (15) are $\pm\lambda_\ell (\ell = 1, 2, 3, 4)$. Assuming the regularity condition, Eq. (7), the solutions of Eqs. (14) and (15) may be written as

$$\tilde{\psi}_1 = \sum_{\ell=1}^{3} A_\ell \mathrm{e}^{-\lambda_\ell z}, \tag{16}$$

$$\tilde{\phi} = \sum_{\ell=1}^{3} d_\ell A_\ell \mathrm{e}^{-\lambda_\ell z}, \tag{17}$$

$$\tilde{T} = \sum_{\ell=1}^{3} e_\ell A_\ell \mathrm{e}^{-\lambda_\ell z}, \tag{18}$$

$$\tilde{\psi}_2 = A_4 \mathrm{e}^{-\lambda_4 z}, \tag{19}$$

with $A_\ell (\ell = 1, 2, 3, 4)$ being arbitrary constants, and e_ℓ and d_ℓ are mentioned in Appendix B.

5. APPLICATIONS

5.1. Mechanical Sources Acting on the Surface

5.1.1. Case 1: Concentrated Normal Force

When the plane boundary is subjected to a concentrated normal force, $P(r, t)$ takes the form,

$$P(r, t) = \frac{P\delta(r)\delta(t)}{2\pi r}, \tag{20}$$

where P is the magnitude of the force and $\delta()$ is the Dirac delta function.

Using Eqs. (4)–(6) and (10)–(12) in the boundary conditions, Eq. (8), along with Eq. (20) and applying the transforms defined by Eq. (13) and substituting the values of $\tilde{\psi}_1, \tilde{\psi}_2, \tilde{\phi}, \tilde{T}$ from Eqs. (16)–(19), we obtain expressions for the components of displacement, stress, temperature distribution, and change in the volume fraction field which are presented in Appendix C.

5.1.2. Case 2: Normal Force over the Circular Region

A uniform pressure of total magnitude P, applied over a uniform circular region of radius a, is obtained by setting

$$P(r,t)=\frac{P}{\pi a^2}H(a-r)\delta(t), \tag{21}$$

at the boundary condition in Eq. (8).

Using Eqs. (10) and (11) (suppressing the primes) and applying the transforms defined by Eq. (13) on Eq. (21), we get

$$\tilde{P}(\xi,p)=\frac{P}{\pi a}\frac{J_1(a\xi)}{\xi}.$$

The expressions for the components of displacement, stress, temperature distribution, and change in volume fraction field can be obtained by replacing R_1 with $(P/\pi a)(J_1(a\xi)/\xi)$ in Eq. (C.1).

5.1.3. Particular Case

If we neglect the effect of voids, i.e., $(\alpha=b=\xi_1=\omega_0=m=\chi=0)$ in Eq. (C.1), we obtain the components of displacement, stress, and temperature distribution in a thermoelastic half-space as mentioned in Appendix D.

By replacing R_1 with $(P/\pi a)(J_1(a\xi)/\xi)$, in Eq. (D.1), we obtain the corresponding expressions for thermoelastic half-space when a normal force is applied over a circular region.

5.2. Thermoelastic Interactions due to Thermal Source

5.2.1. Case 1: Thermal Point Source

When the plane boundary is subjected to a thermal point source, $P(r,t)$ takes the form as

$$P(r,t)=\frac{P\delta(r)\delta(t)}{2\pi r}, \tag{22}$$

where P is the magnitude of the constant temperature applied on the boundary.

Using Eqs. (4)–(6) and (10)–(12) in the boundary conditions, Eq. (9), along with Eq. (22) and applying the transforms defined by Eq. (13) and substituting the values of $\tilde{\psi}_1,\tilde{\psi}_2,\tilde{\phi},\tilde{T}$ from Eqs. (16)–(19), we obtain the expressions for the components of displacement, stress, temperature distribution, and change in volume fraction field by replacing $\Delta_\ell(\ell=1,2,3,4)$ with $-\Delta_\ell'(\ell=1,2,3,4)$, respectively, in Eq. (C.1)

where

$$\Delta_1' = -\{s_4\lambda_2\lambda_3(d_3 - d_2) + n_1(s_2\lambda_3 d_3 - s_3\lambda_2 d_2)\},$$
$$\Delta_2' = s_4\lambda_1\lambda_3(d_3 - d_1) + n_1(s_1\lambda_3 d_3 - s_3\lambda_1 d_1),$$
$$\Delta_3' = -\{s_4\lambda_1\lambda_2(d_2 - d_1) + n_1(s_1\lambda_2 d_2 - s_2\lambda_1 d_1)\},$$
$$\Delta_4' = s_1\lambda_2\lambda_3(d_3 - d_2) + s_2\lambda_1\lambda_3(d_1 - d_3) + s_3\lambda_1\lambda_2(d_2 - d_1).$$

On replacing Δ by $(T_0\omega_1^*/c_1)\Delta_1^*$ and $T_0\Delta_2^*$, respectively, in Eq. (C.1), we obtain the expressions for temperature gradient boundary and temperature input boundary.

5.2.2. Case 2: Thermal Source over the Circular Region

A thermal source of magnitude P applied over a uniform circular region of radius a is obtained by setting

$$P(r, t) = \frac{P\,H(a - r)\delta(t)}{\pi a^2}, \tag{23}$$

in the boundary condition in Eq. (9).

Using Eqs. (10) and (11) (suppressing the primes) and applying the transforms defined by Eq. (13) on Eq. (23), we get

$$\tilde{P}(\xi, p) = \frac{P J_1(a\xi)}{\pi a\xi}. \tag{24}$$

The expressions for the components of displacement, stress, temperature distribution, and change in volume fraction field can be obtained by replacing $\Delta_\ell (\ell = 1, 2, 3, 4)$ with $-\Delta_\ell' (\ell = 1, 2, 3, 4)$ and R_1 with $P J_1(a\xi)/\pi a\xi$, in Eq. (C.1).

On replacing Δ by $(T_0\omega_1^*/c_1)\Delta_1^*$ and $T_0\Delta_2^*$, respectively, in Eq. (C.1), we obtain the expressions for the temperature gradient boundary and temperature input boundary.

5.2.3. Particular Case

Neglecting the effect of voids, the expressions for displacement components, stresses, and temperature distribution in a thermoelastic half-space are obtained by replacing $\Delta_\ell^{**} (\ell = 3, 4, 5)$ with $\Delta_\ell^{***} (\ell = 3, 4, 5)$, and $P = 1$ in Eq. (D.1), respectively,

where

$$\Delta_3^{***} = -(s_2^* n_1 + s_3^*\lambda_2^*), \quad \Delta_4^{***} = s_1^* n_1 + s_3^*\lambda_1^*, \quad \Delta_5^{***} = s_2^*\lambda_1^* - s_1^*\lambda_2^*.$$

By replacing R_1 with $PJ_1(a\xi)/\pi a\xi$, and $\Delta_\ell^{**}(\ell=3,4,5)$ with $\Delta_\ell^{***}(\ell=3,4,5)$, in Eq. (D.1), we obtain the corresponding expressions for the thermoelastic half-space when the thermal source is applied over a circular region.

On replacing Δ^{**} by $(T_0\omega_1^*/c_1)\Delta_1^{**}$ and $T_0\Delta_2^{**}$ in Eq. (D.1), we obtain expressions for the temperature gradient boundary and temperature input boundary, respectively.

Sub-case 1: If $h \to 0$ in Eq. (C.1), we obtain corresponding expressions of displacements, stresses, temperature distribution, and change in volume fraction field for the insulated boundary.

Sub-case 2: If $h \to \infty$ in Eq. (C.1), we obtain the corresponding expressions of displacements, stresses, temperature distribution, and change in volume fraction field for the isothermal boundary.

Special Case: Taking $\epsilon_1=0$ in Eqs. (C.1) and (D.1), we obtain the corresponding expressions of thermoelastic half-space with and without voids, respectively, for the uncoupled theory of thermoelasticity.

6. INVERSION OF THE TRANSFORMS

To obtain the solution of the problem in the physical domain, we must invert the transforms in Eqs. (C.1) and (D.1), for the two theories, i.e., CT and UCT. These expressions are functions of z, the parameters of Laplace and Hankel transforms p and ξ, respectively, and hence are of the form $\tilde{f}(\xi, z, p)$. To get the function $f(r,z,t)$ in the physical domain, first, we invert the Hankel transform using

$$\hat{f}(r,z,p)=\int_0^\infty \xi\,\tilde{f}(\xi,z,p)J_n(\xi r)\,\mathrm{d}\xi. \tag{25}$$

Now, for fixed values of ξ, r, and z, $\hat{f}(r,z,p)$ in Eq. (25) can be considered as the Laplace transform $\hat{g}(p)$ of $g(t)$. Following Honig and Hirdes [37], the Laplace transformed function $\hat{g}(p)$ can be inverted as given below. The function $g(t)$ can be obtained by using

$$g(t)=\frac{1}{2\pi\mathrm{i}}\int_{C-\mathrm{i}\infty}^{C+\mathrm{i}\infty} \mathrm{e}^{pt}\hat{g}(p)\,\mathrm{d}p, \tag{26}$$

where C is an arbitrary real number greater than all the real parts of the singularities of $\hat{g}(p)$. Taking $p=C+\mathrm{i}y$ we get

$$g(t)=\frac{\mathrm{e}^{Ct}}{2\pi}\int_{-\infty}^{\infty} \mathrm{e}^{\mathrm{i}ty}\hat{g}(C+\mathrm{i}y)\,\mathrm{d}y. \tag{27}$$

Now, taking $e^{-Ct}g(t)$ as $h(t)$ and expanding it as a Fourier series in [0,2L], we obtain the formula,

$$g(t) = g_\infty(t) + E_D,$$

where

$$g_\infty(t) = \frac{C_0}{2} + \sum_{k=1}^{\infty} C_k, \quad 0 \le t \le 2L,$$

and

$$C_k = \frac{e^{Ct}}{L} \mathrm{Re}\left[e^{\frac{ik\pi t}{L}} \hat{g}\left(C + \frac{ik\pi}{L} \right) \right]. \tag{28}$$

E_D is the discretization error and can be made arbitrarily small by choosing C large enough. The values of C and L are chosen according to the criteria outlined by Honig and Hirdes [37].

Since the infinite series in Eq. (28) can be summed up only to a finite number of N terms, the approximate value of $g(t)$ becomes

$$g_N(t) = \frac{C_0}{2} + \sum_{k=1}^{N} C_k, \quad 0 \le t \le 2L. \tag{29}$$

Now, we introduce a truncation error E_T, that must be added to the discretization error to produce the total approximate error in evaluating $g(t)$ using the above formula. To accelerate the convergence, the discretization error and then the truncation error is reduced by using the 'Korrecktur method' and the 'ϵ-algorithm,' respectively, as given by Honig and Hirdes [37].

The Korrecktur method formula, to evaluate the function $g(t)$ is

$$g(t) = g_\infty(t) - e^{-2CL} g_\infty(2L + t) + E'_D,$$

where

$$|E'_D| \ll |E_D|.$$

Thus, the approximate value of $g(t)$ becomes

$$g_{N_K}(t) = g_N(t) - e^{-2CL} g_{N'}(2L + t), \tag{30}$$

where N' is an integer such that $N' < N$.

We shall now describe the ϵ-algorithm, which is used to accelerate the convergence of the series in Eq. (29). Let N be an odd natural number and $S_m = \sum_{k=1}^{m} C_k$ be the sequence of partial sums of Eq. (29). We define the'ϵ-sequence' by

$$\epsilon_{0,m} = 0, \quad \epsilon_{1,m} = S_m, \quad \epsilon_{n+1,m} = \epsilon_{n-1,m+1} + \frac{1}{\epsilon_{n,m+1} - \epsilon_{n,m}}; \quad n, m = 1, 2, 3, \ldots$$

The sequence $\epsilon_{1,1}, \epsilon_{3,1}, \ldots, \epsilon_{N,1}$ converges to $g(t) + E_{\mathrm{D}} - \frac{C_0}{2}$ faster than the sequence of partial sums $S_m, m = 1, 2, 3, \ldots$. The actual procedure to invert the Laplace transform consists of Eq. (30) together with the 'ϵ-algorithm'.

The last step is to calculate the integral in Eq. (25). The method for evaluating this integral is described by Press et al. [38], which involves the use of Romberg's integration with an adaptive step size. This, also uses the results from successive refinements of the extended trapezoidal rule followed by extrapolation of the results to the limit when the step size tends to zero.

7. NUMERICAL RESULTS AND DISCUSSION

Following Dhaliwal and Singh [39], we take the case of magnesium crystal-like material for numerical calculations. The physical constants used are

$\lambda = 2.17 \times 10^{10}\,\mathrm{N{\cdot}m^{-2}}$, $\mu = 3.278 \times 10^{10}\,\mathrm{N{\cdot}m^{-2}}$, $\rho = 1.74 \times 10^{3}\,\mathrm{kg{\cdot}m^{-3}}$,
$c_e = 1.04 \times 10^{3}\,\mathrm{J{\cdot}kg^{-1}{\cdot}K^{-1}}$, $\omega_1^* = 3.58 \times 10^{11}\,\mathrm{s^{-1}}$, $P = 1$, $T_0 = 298\,\mathrm{K}$,
$K = 1.7 \times 10^{2}\ \mathrm{W{\cdot}m^{-1}{\cdot}K^{-1}}$, $\beta = 2.68 \times 10^{6}\,\mathrm{N{\cdot}m^{-2}{\cdot}K^{-1}}$,

and the void parameters are

$\chi = 1.753 \times 10^{-15}\,\mathrm{m^2}$, $\alpha = 3.688 \times 10^{-5}\,\mathrm{N}$, $\xi_1 = 1.475 \times 10^{10}\,\mathrm{N{\cdot}m^{-2}}$
$b = 1.13849 \times 10^{10}\,\mathrm{N{\cdot}m^{-2}}$, $\omega_0 = 0.0787 \times 10^{-3}\,\mathrm{N{\cdot}m^{-2}{\cdot}s}$,
$m = 2 \times 10^{6}\,\mathrm{N{\cdot}m^{-2}{\cdot}K^{-1}}$.

Figures 1–6 and 8–13 show comparisons of dimensionless normal boundary displacement w, boundary temperature field T, and normal stress t_{zz} with distance r for coupled thermoelasticity with voids (CTV), uncoupled thermoelasticity with voids (UCTV), coupled thermoelasticity without voids (CTWV), uncoupled thermoelasticity without voids (UCTWV) for concentrated source (CS) and source over circular region (SCR). Figures 7 and 14 depict the change in the volume fraction field ϕ with distance r for both sources. The computations are carried out for dimensionless time $t = 1.0$ and $t = 2.0$ at $z = 1.0$ in the range $0 \le r \le 10$.

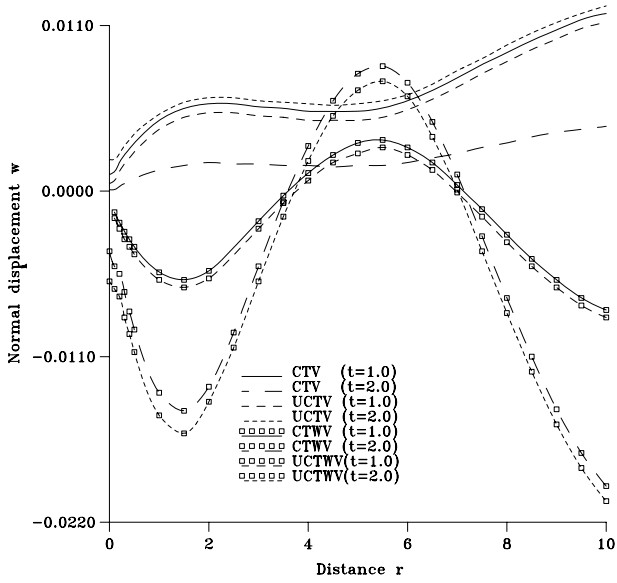

Fig. 1. Variation of the normal displacement w with distance r (concentrated normal force).

The solid and dashed lines with center symbols are denoted by CTWV and UCTWV; those without center symbols are denoted by CTV and UCTV, respectively. In Fig. 7 the solid and dashed lines without center symbols correspond to a concentrated source for coupled thermoelasticity (CSCT) and a concentrated source for uncoupled thermoelasticity (CSUCT), respectively, and in Fig. 14 the solid and dashed lines with center symbols correspond to a source over the circular region for coupled thermoelasticity (SCRCT) and a source over the circular region for uncoupled thermoelasticity (SCRUCT), respectively. The results for a source over a circular region are presented for a dimensionless width $a = 1$.

7.1. Normal Force on the Boundary of Half-Space (Insulated Boundary)

7.1.1. Case 1: Concentrated Normal Force

Figure 1 depicts the variation of the normal displacement w with distance r. At the point of application of the source, the values of the normal displacement w for CTV and UCTV are greater than for CTWV and UCTWV at time $t = 1.0$ and $t = 2.0$. Due to the presence of voids, the values of w for CTV and UCTV increase slowly with an increase in distance r in the range $0 \leq r \leq 10$ at time $t = 1.0$ and $t = 2.0$. The values of

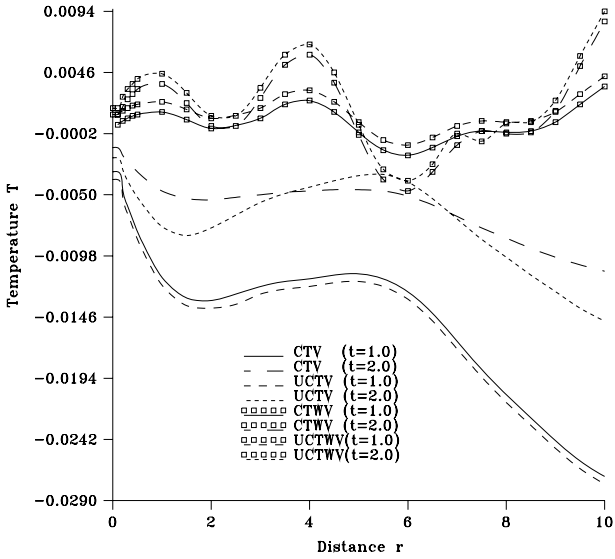

Fig. 2. Variation of the temperature distribution T with distance r (concentrated normal force).

w decrease in the ranges, $0 \leq r \leq 2$ and $5 \leq r \leq 10$, and increase in the rest of the ranges for both theories.

Figure 2 shows the variation of the temperature distribution T with distance r. Initially the values of T for CTWV and UCTWV are larger than for CTV and UCTV at times $t = 1.0$ and $t = 2.0$. The values of T for UCTV at time $t = 1.0$ are less than CTV at time $t = 1.0$ and $t = 2.0$ and UCTV at time $t = 2.0$.

Figure 3 shows the variation of the normal stress t_{zz} with distance r. The values of t_{zz} show opposite oscillatory behavior for CTV, UCTV and CTWV, UCTWV at times $t = 1.0$ and 2.0 over the whole range.

7.1.2. Case 2: Normal Force over the Circular Region

The values of the normal displacement w, temperature distribution T, and normal stress t_{zz} show opposite oscillatory behavior for CTV, UCTV and CTWV, UCTWV at times $t = 1.0$ and 2.0 in the range $0 \leq r \leq 10$. These variations are shown in Figs. 4–6, respectively.

Figure 7 depicts the variation of change in the volume fraction field ϕ with distance r. The values of ϕ decrease slowly with an increase in distance r when the concentrated force is applied for both theories and for both values of time. If we fix the point of observation, i.e., the distance r, the values of ϕ increase or decrease with the passage of time for the case when the force is applied over the circular region for the two theories.

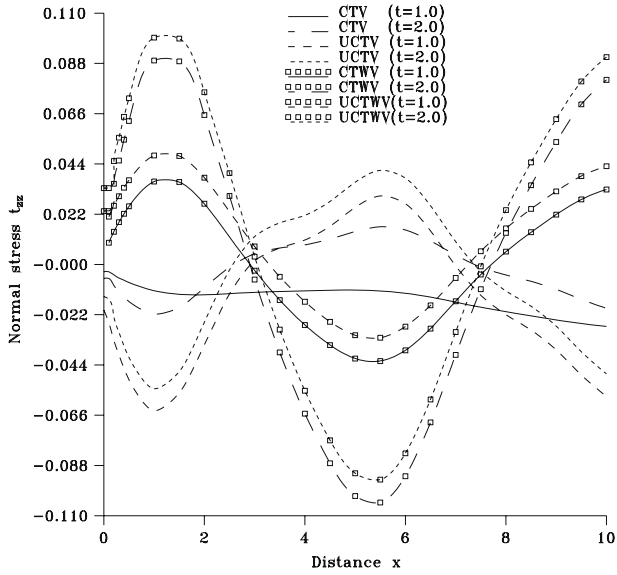

Fig. 3. Variation of the normal stress t_{zz} with distance r (concentrated normal force).

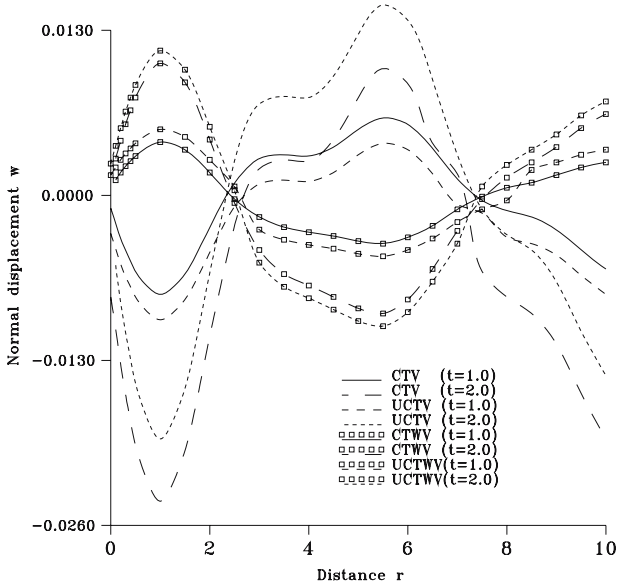

Fig. 4. Variation of the normal displacement w with distance r (normal force over the circular region).

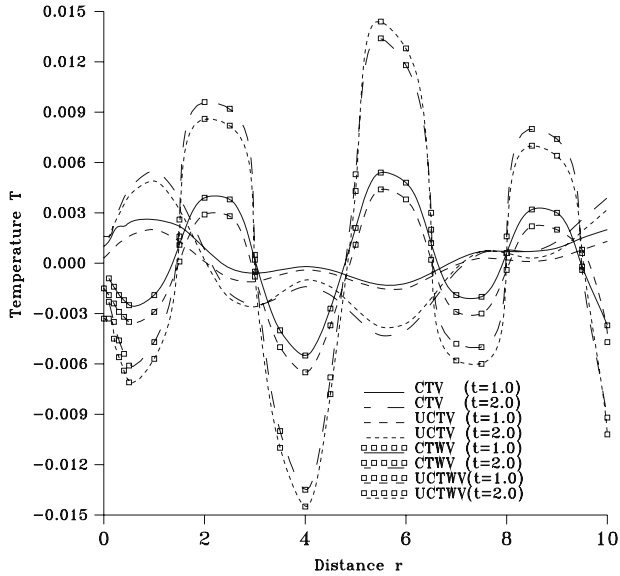

Fig. 5. Variation of the temperature distribution T with distance r (normal force over the circular region).

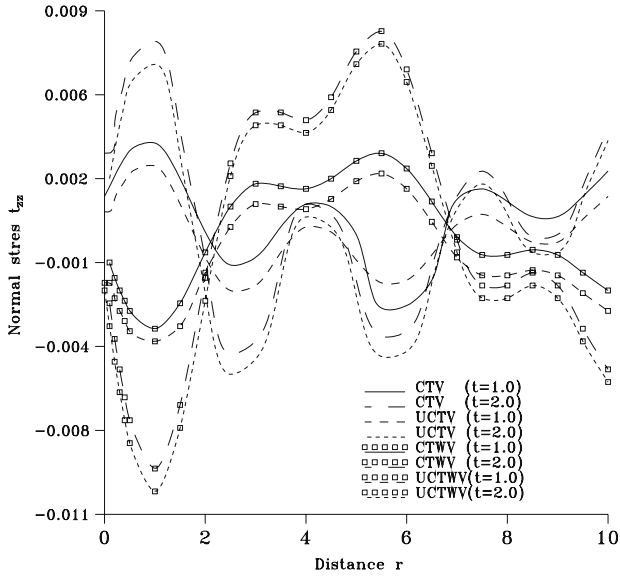

Fig. 6. Variation of the normal stress t_{zz} with distance r (normal force over the circular region).

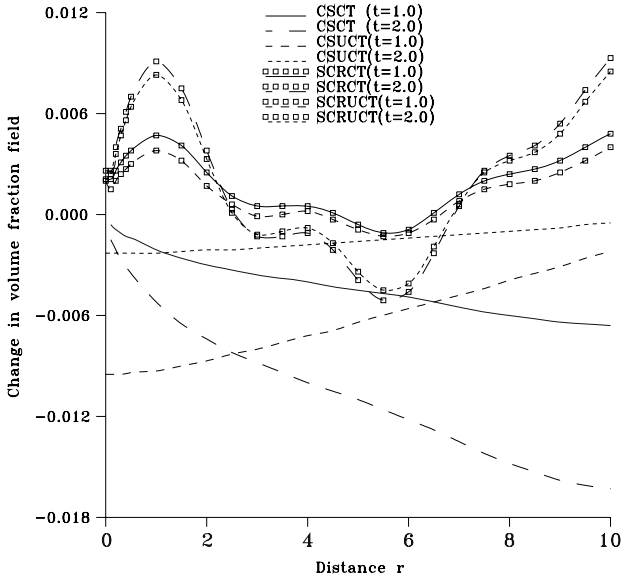

Fig. 7. Variation of change in the volume fraction field ϕ with distance r (normal force).

7.2. Thermal Source on the Surface of Half-Space (Temperature Gradient Boundary)

7.2.1. Case 1: Thermal Point Source

Figure 8 shows the variation of the normal displacement w with the distance r. Due to the presence of voids, the values of w decrease sharply and then become oscillatory over the whole range for both theories and for times $t = 1.0$ and $t = 2.0$. For CTWV the values of w depict very small variation about zero in the range $0 \leq r \leq 5$ and increase slowly over the rest of the range for both values of time. A similar trend of variation is observed as for CTWV as for UCTWV.

Figure 9 depicts the variation of the temperature distribution T with distance r. Due to the effect of the voids, the values of T show very small variation in the whole range for both the theories and for both values of times. At time $t = 2.0$ the values of T for CTWV and UCTWV are greater than those for time $t = 1.0$ in the ranges, $0 \leq r \leq 2, 6 \leq r \leq 10$, and less in the rest of the ranges

Figure 10 shows the variation of the normal stress t_{zz} with distance r. Due to the presence of voids, the values of t_{zz} show small variations about zero for both theories and for both values of time. At times $t = 1.0$ and

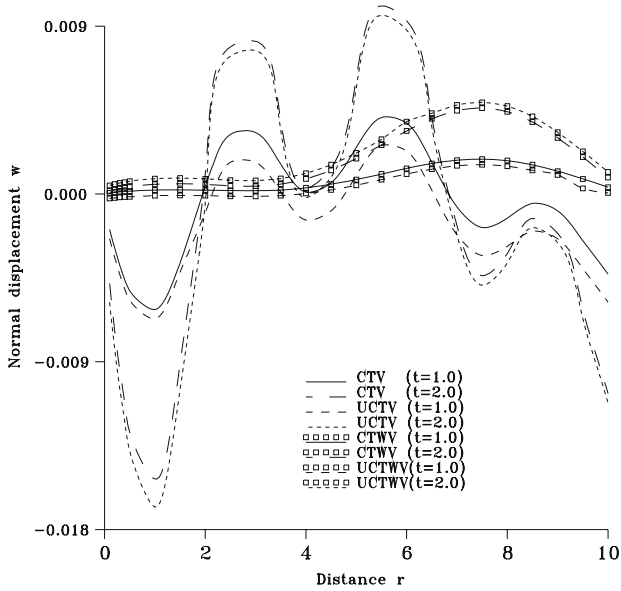

Fig. 8. Variation of the normal displacement w with distance r (thermal point source).

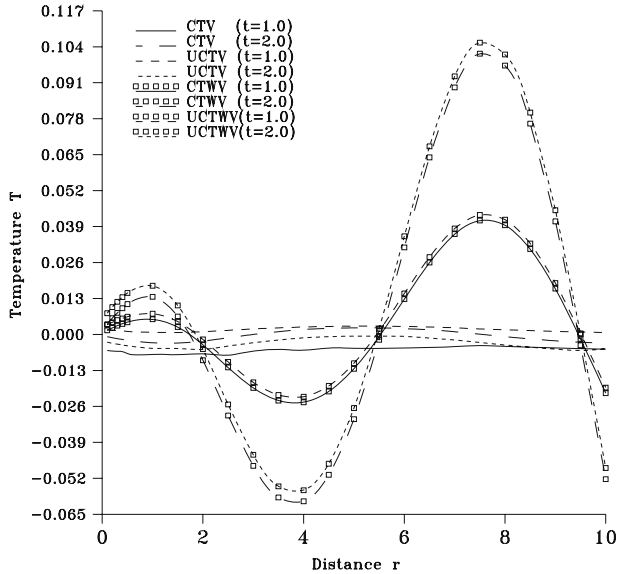

Fig. 9. Variation of the temperature distribution T with distance r (thermal point source).

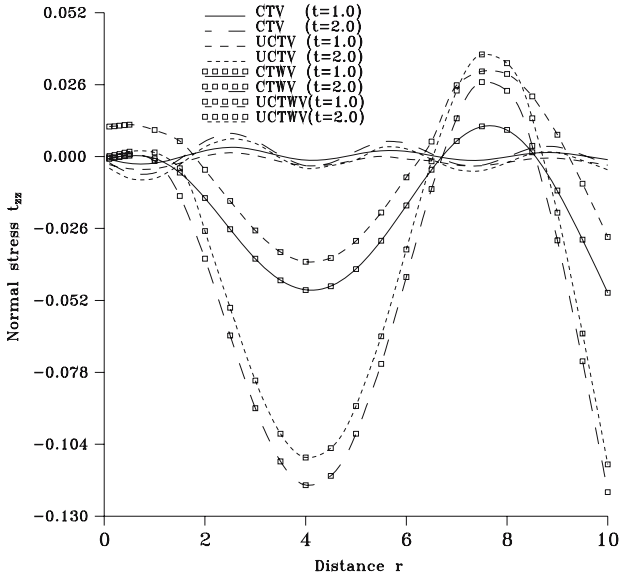

Fig. 10. Variation of the normal stress t_{zz} with distance r (thermal point source).

2.0, the values for UCTWV are greater than for CTWV in the range $0 \leq r \leq 10$.

7.2.2. Case 2: Thermal Source over the Circular Region

Figure 11 depicts the variation of the normal displacement w with distance r. Due to the presence of voids, the values of w show the same oscillatory pattern about zero over the whole range for both theories and for both values of time. For CTWV and UCTWV the values of w initially decrease slowly and then become oscillatory in the range $0 \leq r \leq 10$ for times $t = 1.0$ and $t = 2.0$.

The values of the temperature distribution T show the opposite oscillatory behavior for CTV, UCTV and CTWV, UCTWV at times t = 1.0 and 2.0 in the range $0 \leq r \leq 10$. The values of the normal stress t_{zz} show the same oscillatory behavior in the ranges $0 \leq r \leq 3$ and $6.5 \leq r \leq 9$ and the opposite in the rest of the ranges. These variations are shown in Figs. 12 and 13, respectively.

Figure 14 depicts the variation of change in the volume fraction field ϕ with distance r. The values of ϕ are observed to follow the same oscillatory pattern about zero over the whole range for both sources and for both values of time.

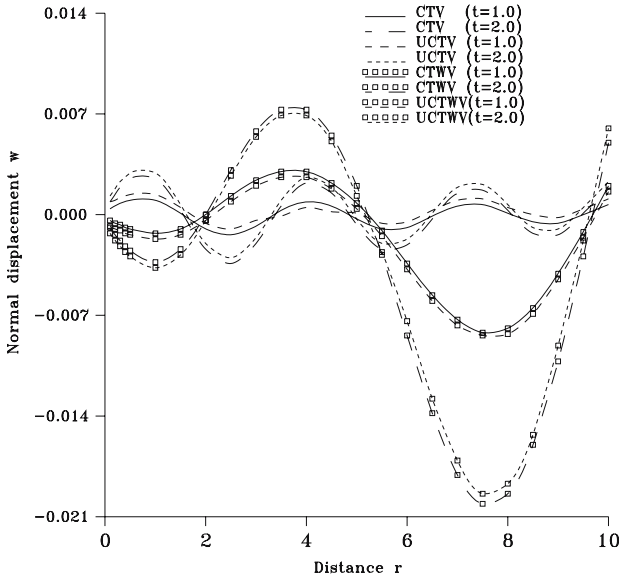

Fig. 11. Variation of the normal displacement w with distance r (source over the circular region).

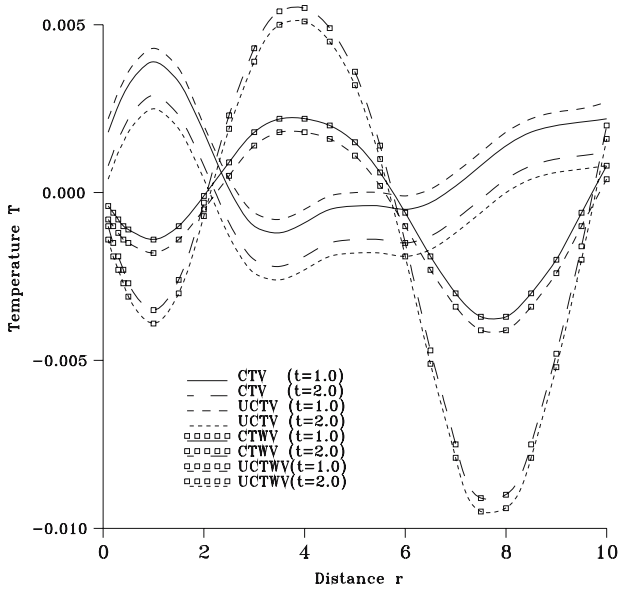

Fig. 12. Variation of the temperature distribution T with distance r (source over the circular region).

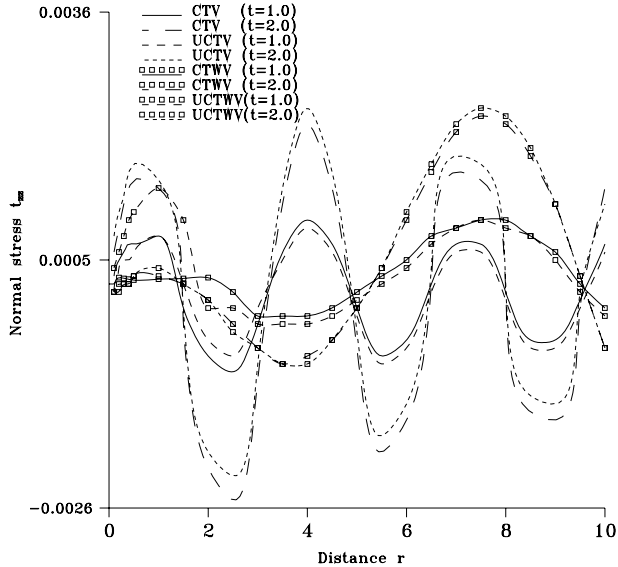

Fig. 13. Variation of the normal stress t_{zz} with distance r (source over the circular region).

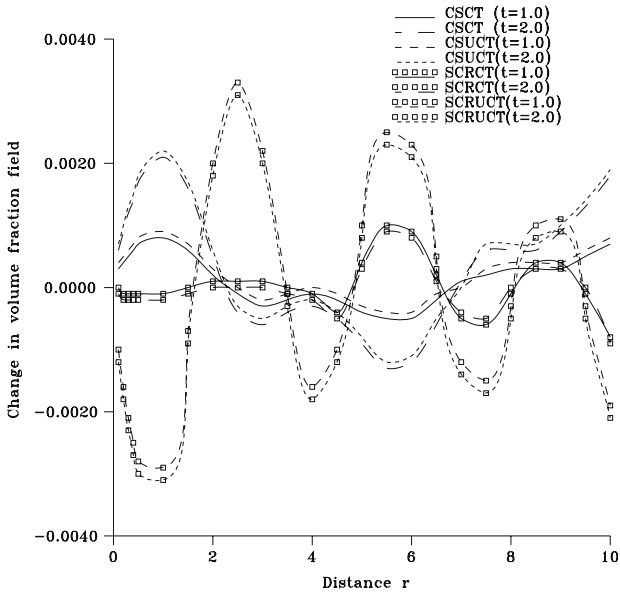

Fig. 14. Variation of change in the volume fraction field ϕ with distance r (thermal source).

8. CONCLUSIONS

(a) The two-dimensional axi-symmetric problem in a homogeneous, isotropic, thermoelastic half-space with voids due to normal force and thermal source has been analyzed.
(b) The Laplace and Hankel transform technique is used to derive the components of displacement, stress, temperature distribution, and change in volume fraction field.
(c) It is observed that with an increase in the radial distance, that is, the distance of the point of observation from the point of application of the source, for each value of time, the numerical absolute values of the normal displacement, normal stress, and temperature distribution generally follow oscillatory patterns about zero over the whole range.
(d) The effect of voids on the normal displacement, normal stress, and temperature distribution has been depicted graphically for the magnesium crystal for the two theories for an insulated boundary and a temperature gradient boundary.

Appendix A. COEFFICIENTS OF EQ. (14)

$$Q = -\frac{1}{b_1}\{b_1(b_2+b_3)+(a_4+b_1\xi^2)-a_2a_5+a_3\in_1 p\},$$

$$N = \frac{1}{b_1}\{(\,b_2b_3+a_8a_{10})b_1+(a_4+b_1\xi^2)(b_2+b_3)-a_5(a_2b_3+a_3a_{10})-a_2a_5\xi^2 - \in_1 p(a_2a_8-a_3b_2)+a_3\in_1 p\xi^2\},$$

$$I = -\frac{1}{b_1}[(b_1\xi^2+a_4)(b_2b_3+a_8a_{10})+a_5\xi^2(a_2b_3+a_3a_{10}) + \in_1 p\xi^2(a_2a_8-a_3b_2)],$$

$$b_1 = (1+a_1), \quad b_2=\xi^2+a_6+a_7+a_9, \quad b_3=\xi^2+\frac{\rho c_e c_1^2 p}{K\omega_1^*},$$

$$a_1=\frac{\mu}{\lambda+\mu}, \quad a_2=\frac{bc_1^2}{(\lambda+\mu)\chi\omega_1^{*2}}, \quad a_3=\frac{\beta T_0}{\lambda+\mu}, \quad a_4=\frac{\rho c_1^2 p^2}{(\lambda+\mu)},$$

$$a_5=\frac{b\chi}{\alpha}, \quad a_6=\frac{\xi_1 c_1{}^2}{\omega_1^{*2}\alpha}, \quad a_7=\frac{\omega_0 c_1^2 p}{\omega_1^*\alpha}, \quad a_8=\frac{m\chi T_0}{\alpha},$$

$$a_9=\frac{\rho\chi c_1^2}{\alpha}p^2, \quad a_{10}=\frac{mc_1^4 p}{\omega_1^{*3}\chi K}.$$

Appendix B. COEFFICIENTS OF EQS. (17) and (18)

$$e_\ell = \frac{U^*\lambda_\ell^2 + V^*}{W^* + a_{10}^{-1}\lambda_\ell^2}, \qquad d_\ell = \frac{P^*\lambda_\ell^2 + Q^*}{R^* - a_8^{-1}\lambda_\ell^2}; \quad (\ell = 1, 2, 3),$$

$$U^* = \frac{\in_1 p}{a_{10}} - \frac{b_1}{a_2}, \qquad V^* = \frac{b_1\xi^2}{a_2} + \frac{a_4}{a_2} - \frac{\in_1 p\xi^2}{a_{10}},$$

$$W^* = -\left(\frac{a_3}{a_2} + \frac{b_3}{a_{10}}\right), \qquad P^* = \frac{b_1}{a_3} - \frac{a_5}{a_8},$$

$$Q^* = \frac{(\xi^2 b_1 + a_4)}{a_3} - \frac{a_4\xi^2}{a_6}, \qquad R^* = \frac{b_2}{a_8} - \frac{a_2}{a_3}.$$

Appendix C. EXPRESSIONS FOR THE COMPONENTS OF DISPLACEMENTS, STRESSES, TEMPERATURE DISTRIBUTION, AND CHANGE IN VOLUME FRACTION FIELD FOR THERMOELASTIC BODY WITH VOIDS

$$\tilde{u} = -\left[\xi R_1 \left\{\sum_{\ell=1}^{3} \Delta_\ell e^{-\lambda_\ell z} - (\lambda_4 \Delta_4 e^{-\lambda_4 z})\right\}\right] \Big/ \Delta,$$

$$\tilde{w} = -\left[R_1 \left\{\sum_{\ell=1}^{3} \lambda_\ell \Delta_\ell e^{-\lambda_\ell z} - (\xi^2 \Delta_4 e^{-\lambda_4 z})\right\}\right] \Big/ \Delta,$$

$$\tilde{T} = \left[R_1 \left(\sum_{\ell=1}^{3} e_\ell \Delta_\ell e^{-\lambda_\ell z}\right)\right] \Big/ \Delta,$$

$$\tilde{t}_{zz} = \left[R_1 \left(\sum_{\ell=1}^{4} s_\ell \Delta_\ell e^{-\lambda_\ell z}\right)\right] \Big/ \Delta,$$

$$\tilde{t}_{zr} = \left[R_1 \left\{\sum_{\ell=1}^{3} \lambda_\ell \Delta_\ell e^{-\lambda_\ell z} - (n_1 \Delta_4 e^{-\lambda_4 z})\right\}\right] \Big/ \Delta,$$

$$\tilde{\phi} = \left[R_1 \left(\sum_{\ell=1}^{3} d_\ell \Delta_\ell e^{-\lambda_\ell z}\right)\right] \Big/ \Delta, \tag{C.1}$$

where

$$\Delta = \Delta_1^* + h\Delta_2^*,$$

$$\Delta_1^* = \lambda_2\lambda_3\,(s_4\lambda_1 - n_1 s_1)\,(d_3e_2 - d_2e_3) + \lambda_1\lambda_3\,(s_4\lambda_2 + n_1 s_2)\,(d_1e_3 + e_1d_3) + \lambda_1\lambda_2\,(s_4\lambda_3 + n_1 s_3)\,(d_1e_2 - e_1d_2)\,,$$

$$\Delta_2^* = (s_4\lambda_1 - n_1 s_1)\,(e_3\lambda_2 d_2 - e_2 d_3\lambda_3) + (e_3\lambda_1 d_1 - e_1\lambda_3 d_3)\,(s_4\lambda_2 + n_1 s_2) + (s_4\lambda_3 + n_1 s_3)\,(e_1\lambda_2 d_2 - e_2\lambda_1 d_1)\,,$$

$$\Delta_1 = n_1\{\lambda_2\lambda_3\,(d_3e_2 - d_2e_3) + h(\lambda_2 d_2 e_3 - \lambda_3 d_3 e_2)\},$$

$$\Delta_2 = -n_1\{\lambda_1\lambda_3\,(d_3e_1 - d_1e_3) + h(\lambda_1 d_1 e_3 - \lambda_3 d_3 c_1)\},$$

$$\Delta_3 = -n_1\{\lambda_1\lambda_2\,(d_2e_1 - d_1e_2) + h(\lambda_1 d_1 e_2 - \lambda_2 d_2 e_1)\},$$

$$\Delta_4 = [\lambda_1\lambda_2\lambda_3\{e_3\,(d_1 - d_2) + e_2\,(d_3 - d_1) + e_1\,(d_2 - d_3)\} + h\{\lambda_1(\lambda_2 d_2 e_3 - \lambda_3 d_3 e_2) - \lambda_2(\lambda_1 d_1 e_3 - \lambda_3 d_3 e_1) + \lambda_3(\lambda_1 d_1 e_2 - \lambda_2 d_2 e_1)\},$$

$$s_\ell = s'_{10} + \lambda_\ell^2 s'_{20} + d_\ell s'_{30} + e_\ell; \quad (\ell = 1, 2, 3), \quad s_4 = -(s'_{10} + \xi^2 s'_{20})\lambda_4,$$

$$s'_{10} = -\frac{\lambda\xi^2}{\beta T_0}, \quad s'_{20} = \frac{(\lambda+2\mu)}{\beta T_0}, \quad s'_{30} = \frac{bc_1^2}{\beta T_0 \omega_1^{*2}\chi},$$

$$s'_{10} = -\frac{\lambda\xi^2}{\beta T_0}, \quad s'_{20} = \frac{(\lambda+2\mu)}{\beta T_0}, \quad s'_{30} = \frac{bc_1^2}{\beta T_0 \omega_1^{*2}\chi},$$

$$R_1 = \frac{P}{2\pi}, \quad \lambda_4 = \left(\frac{a_1\xi^2 + a_4}{a_1}\right)^{\frac{1}{2}}, \quad n_1 = \frac{\lambda_4^2 + \xi^2}{2}.$$

Appendix D. EXPRESSIONS FOR THE COMPONENTS OF DISPLACEMENTS, STRESSES, TEMPERATURE DISTRIBUTION, AND CHANGE IN VOLUME FRACTION FIELD FOR THERMOELASTIC BODY WITHOUT VOIDS

$$\tilde{u} = -[R_1\xi\{(\Delta_3^{**}\mathrm{e}^{-\lambda_1^* z} + \Delta_4^{**}\mathrm{e}^{-\lambda_2^* z}) - \Delta_5^{**}\lambda_4\mathrm{e}^{-\lambda_4^z}\}]/\Delta^{**},$$

$$\tilde{w} = [R_1\{\lambda_1^*\Delta_3^{**}\mathrm{e}^{-\lambda_1^* z} + \lambda_2^*\Delta_4^{**}\mathrm{e}^{-\lambda_2^* z} + \xi^2\Delta_5^{**}\mathrm{e}^{-\lambda_4^z}\}]/\Delta^{**},$$

$$\tilde{t}_{zz} = [R_1\{s_1^*\Delta_3^{**}\mathrm{e}^{-\lambda_1^* z} + s_2^*\Delta_4^{**}\mathrm{e}^{-\lambda_2^* z} + s_3^*\Delta_5^{**}\mathrm{e}^{-\lambda_4^z}\}]/\Delta^{**},$$

$$\tilde{t}_{zr} = -[R_1\{\lambda_1^*\Delta_3^{**}\mathrm{e}^{-\lambda_1^* z} + \lambda_2^*\Delta_4^{**}\mathrm{e}^{-\lambda_2^* z} - n_1\Delta_5^{**}\mathrm{e}^{-\lambda_4^z}\}]/\Delta^{**},$$

$$\tilde{T} = -[R_1\{e_1^*\Delta_3^{**}\mathrm{e}^{-\lambda_1^* z} + e_2^*\Delta_4^{**}\mathrm{e}^{-\lambda_2^* z}\}]/\Delta^{**}, \tag{D.1}$$

where

$$\Delta^{**} = \Delta_1^{**} + h\Delta_2^{**},$$
$$\Delta_1^{**} = -\left(s_1^* e_2^* \lambda_2^* - s_2^* e_1^* \lambda_1^*\right) n_1 + \left(e_1^* - s_3^* e_2^*\right) \lambda_1^* \lambda_2^*,$$
$$\Delta_2^{**} = \left(s_1^* e_2^* - s_2^* e_1^*\right) n_1 + s_3^* e_2^* \lambda_1^* - e_1^* \lambda_2^*,$$
$$\Delta_3^{**} = -(\lambda_2^* - h) e_2^* n_1,$$
$$\Delta_4^{**} = -(\lambda_1^* - h) e_1^* n_1,$$
$$\Delta_5^{**} = -\{(e_1^* - e_2^*)\lambda_1^* \lambda_2^* + h(e_2^* \lambda_1^* - \lambda_2^* e_1^*)\},$$
$$\lambda_\ell^{*2} = \frac{-A + (-1)^{\ell+1}\sqrt{A^2 - 4B}}{2}; \quad \ell = 1, 2.$$

$$A = -\frac{(\xi^2 b_1 + a_4) + b_1 b_3 + a_3 \in_1 p}{b_1}, \quad B = \frac{(\xi^2 b_1 + a_4) b_3 + a_3 \in_1 p \xi^2}{b_1},$$
$$s_\ell^* = s_{10}' + \lambda_\ell^{*2} s_{20}' + e_\ell^*; \quad (\ell = 1, 2), \quad s_3^* = \xi^2 s_{20}' \lambda_4,$$
$$e_\ell^* = \frac{b_1 \lambda_\ell^{*2} - (a_4 + b_1 \xi^2)}{b_2}; \quad \ell = 1, 2.$$

REFERENCES

1. J. W. Nunziato and S. C. Cowin, *Arch. Rational Mech. Anal.* **72**:175 (1979).
2. S. C. Cowin and J. W. Nunziato, *J. Elasticity* **13**:125 (1983).
3. P. Puri and S. C. Cowin, *J. Elasticity* **15**:167 (1985).
4. R. S. Dhaliwal and J. Wang, *Int. J. Eng. Sci.* **32**:1823 (1994)
5. E. Scarpetta, *Int. J. Eng. Sci.* **33**:151 (1995).
6. M. Birsan, *Libertas Math.* **20**:95 (2000).
7. M. Ciarletta, G. Iovane, and M. A. Sumbatyan, *Int. J. Eng. Sci.* **41**:246 (2003).
8. G. Rusu, *Bull. Polish Acad. Sci. Tech. Sci.* **35**:339 (1987).
9. G. Saccomandi, *Rend. Mat. Appl.* **12**:45 (1992).
10. M. Ciarletta and A. Scalia, *Z. Angew. Math. Mech.* **73**:67 (1993).
11. M. Ciarletta and E. Scarpetta, *Z. Angew. Math. Mech.* **75**:707 (1995).
12. R. S. Dhaliwal and J. Wang, *Acta Mech.* **110**:33 (1995).
13. M. Marin, *Rend. Mat. Appl.* **17**:103 (1997).
14. M. Marin, *Arch. Math. (Brno)* **33**:301 (1997).
15. M. Marin, *Cienc. Mat. (Havana)* **16**:101 (1998).
16. M. Marin and H. Salca, *Theoret. Appl. Mech.* **24**:99 (1998).
17. S. Chirita and A. Scalia, *J. Therm. Stresses* **24**:433 (2001).
18. A. Pompei and A. Scalia, *J. Therm. Stresses* **25**:183 (2002).
19. A. Scalia, A. Pompei, and S. Chirita, *J. Therm. Stresses* **27**:209 (2004).
20. M. C. Wadhawan, *Pageoph* **102**:37 (1973).
21. A. H. Ghosen and M. Sabbaghia, *J. Therm. Stresses* **5**:299 (1982).
22. A. Chattopadhyay, A. Keshri, and S. Base, *Indian J. Appl. Math.* **16**:807 (1985).
23. Y. C. Yang, T. S. Wang, and C. K. Chen, *J. Therm. Stresses* **9**:19 (1986).
24. N. Noda, *J. Therm. Stresses* **10**:57 (1987).

25. M. Kurashige, *Trans. JSME Ser. A* **57**:2672 (1991).
26. D. S. Chandrasekharaiah and H. R. Keshavan, *Acta Mech.* **92**:61 (1992).
27. M. A. Ezzat, *Int. J. Eng. Sci.* **33**:2011 (1995).
28. N. Khomasuridze and I. Khomasuridze, *Proc. I. Vekua Inst. Appl. Math.* **48**:44 (1998).
29. A. A Yevtushenko and R. D. Kulchysky-Zhyhailo, *Int. J. Eng. Sci.***37**:1959 (1999).
30. S. Mukhopadhyay and R. N. Mukherjee, *Indian J. Appl. Math.* **35**:635 (2002).
31. M. Rahman, *Int. J. Eng. Sci.* **41**:1899(2003).
32. E. G. Yanyutin and I. V. Yanchevsky, *Int. J. Solids Struct.* **41**:3643 (2004).
33. H. H. Sherief, A. E. M. Elmisiery, and M. A. Elhagary, *J. Therm. Stresses* **27**:885 (2004).
34. A. Baksi, R. K. Bera, and L. Debnath, *Int. J. Eng. Sci.* **42**:1573 (2004).
35. R. Kumar and L. Rani, *J. Therm. Stresses* **28**:123 (2005).
36. W. Nowacki, *Thermoelasticity*, 2nd edn. (Pergamon, PWN-Polish Scientific Pubs., Warsaw, Poland, 1986).
37. G. Honig and U. Hirdes, *J. Comput. Appl. Math.* **10**:113 (1984).
38. W. H. Press, S. A. Teukolshy, W. T. Vellerling, and B. P. Flannery, *Numerical Recipes* (Cambridge University Press, Cambridge, 1986).
39. R. S. Dhaliwal and A. Singh, *Dynamic Coupled Thermoelasticity* (Hindustan Pub. Corp., New Delhi, India, 1980), p. 726.